



Trans. Nonferrous Met. Soc. China 31(2021) 1518-1528

Transactions of Nonferrous Metals Society of China

www.tnmsc.cn



Free dendritic growth model considering both interfacial nonisothermal nature and effect of convection for binary alloy

Shu-cheng LIU¹, Li-hua LIU¹, Shu LI^{2,3}, Jin-zhong WANG¹

- School of Materials Science and Engineering, Harbin Institute of Technology, Harbin 150001, China;
 School of Science, Harbin University of Science and Technology, Harbin 150080, China;
 Heilongjiang Provincial Key Laboratory of Quantum Manipulation & Control,
 - 3. Heilongjiang Provincial Key Laboratory of Quantum Manipulation & Contro Harbin University of Science and Technology, Harbin 150080, China

Received 25 May 2020; accepted 30 December 2020

Abstract: Considering both the effect of the nonisothermal nature of the interface as well as the effect of forced convection, an extended free dendritic growth model for binary alloys was proposed. Comparative analysis indicates that the effect of convection on solute diffusion is more remarkable compared with the ignorable effect of convection on thermal diffusion at low bath undercooling, due to the fact that solute diffusion coefficient is usually three orders of magnitude less than thermal diffusion coefficient. At high bath undercooling, the effect of convection on the dendritic growth is very slight. Furthermore, a satisfying agreement between the model predictions with the available experiment data for the $Cu_{70}Ni_{30}$ alloy was obtained, especially at low bath undercoolings, profiting from the higher values of interfacial migration velocity predicted by the present model with nonideal fluid case than that predicted by the one ignoring the effect of convection.

Key words: modeling; dendritic solidification; binary alloys; nonisothermal interface; convection

1 Introduction

Theoretical analysis mathematical and modeling implicated in the investigation of crystal are as important as experimental observation [1-6]. To describe the free dendritic growth, three aspects should be taken into account, which are the interface kinetics, the thermal or solutal transport in the bulk liquid ahead of the solid-liquid interface and the morphological stability for the interface [7-14]. The interface kinetics, i.e. the interface response function [15], is used to set up a relationship between the interfacial migration velocity and thermodynamic driving force determined by the interfacial temperature and compositions of solid and liquid phases. The thermal or solutal transport in liquid is commonly dealt with by solving the classical Fick diffusion equation or the extended hyperbolic diffusion equation [16,17]. The morphological stability analysis should also be made, which gives a relationship between the interfacial migration velocity and the dentritic tip radius of curvature [18].

Most of the free dendritic growth models have a deficiency, i.e. the isothermal and isosolutal solid-liquid interface assumption. In fact, the interface is nonisothermal and nonisosolutal one [19]. Strictly speaking, the solid-liquid interface is non-planar one, which leads to the variable interfacial curvature and normal velocity along the curved interface. Additionally, the crystalline anisotropy results in the interfacial

energy anisotropy and the kinetic growth anisotropy. Recently, for eliminating the isothermal and isosolutal solid-liquid interface assumption, LI et al [20–24] have successfully obtained the exact solution of steady state Fick diffusion equation and made a series of comparative analysis. It was further demonstrated that the effect of the nonisothermal nature of interface is significant and the effect of the nonisosolutal nature of interface is very slight and really negligible.

Those models [20–24], however, ignore the influence of convection on dendrite growth. It is interesting and necessary to consider convection effect when modeling the free dendrite growth [25–28]. There are two kinds of convection, i.e., the forced convection and the natural convection. The forced convection is caused by an external force. The natural convection occurs naturally and is caused by the density change due to the variation in concentration or temperature. In the present work, the focus of our attention is the forced convection to model the free dentritic growth during solidification. The forced convection affects the thermal or solutal transport in the liquid as well as morphological stability for the interface. According to the Navier-Stokes equation [26,28], the new thermal diffusion equation was re-solved. Based on microscopic solvability theory, the tip radius of dendrite given by ALEXANDROV and GALENKO [28-31] was adopted. Comparisons with the related models and the available experiment data were also made.

2 Modeling

In this section, considering a forced convection in alloy melts, the thermal diffusion equations with the nonisothermal boundary condition were re-solved to discuss the influence of convection on thermal diffusion. The results for solutal transport and morphological stability criterion given by ALEXANDROV and GALENKO [28] were adopted considering convection and isosolutal interface assumption.

2.1 Thermal transport in liquid

Crystal growth in the incoming flow of fluid is described in terms of the nonlinear Stefan type diffusion problem [32,33] with the moving free boundary of phase transition. The flow can be

described by the Navier-Stokes equation [26,28]:

$$(\boldsymbol{\omega} \cdot \nabla)\boldsymbol{\omega} = -\frac{1}{\rho} \nabla P + \eta \nabla^2 \boldsymbol{\omega}, \ \nabla \cdot \boldsymbol{\omega} = 0$$
 (1)

where ω is the fluid flow velocity, ∇ is the vector gradient operator, ρ is the density, P is the pressure, and η is the kinematic viscosity of the fluid. Considering convection in the liquid and ignoring diffusion in the solid, the thermal transport phenomena can be described by the extended Fick diffusion equation as

$$\frac{\partial T_{\rm L}}{\partial t} + (\boldsymbol{\omega} \cdot \nabla) T_{\rm L} = D_{\rm T} \nabla^2 T_{\rm L} \tag{2}$$

where T_L is the temperature in bulk liquid, t is time, and D_T is the thermal diffusivity in the liquid.

In a small domain of the tip, the solid-liquid interface can be approximated by a paraboloid of revolution under the steady state dendritic growth condition in undercooled melts [18,34]. It is convenient to use a parabolic coordinate system (α, β, φ) to solve temperature and solute fields in the liquid phase, instead of the Cartesion coordinate system (x, y, z). The coordinate transition is adopted: $x=r\alpha\beta\cos\varphi$, $y=r\alpha\beta\sin\varphi$, and $z'=0.5r(\alpha^2-\beta^2)$, where r is the tip radius of curvature, z'=z-Vt is a conversion to fix the reference frame on the moving interface, and V is the interfacial migration velocity in the z-direction. Then $\alpha=1$ represents the solid-liquid interface with a tip radius of curvature r [22]. The temperature and solute concentration fields in the bulk liquid have the forms $T_L(\alpha, \beta)$ and $C_{\rm L}(\alpha, \beta)$, respectively. Here, the coordinate φ is not included due to rotational symmetry. With the parabolic coordinate system (α, β, φ) , Eq. (2) is rewritten as follows [28]:

$$u_{\alpha}\alpha \frac{\partial T_{L}}{\partial \alpha} + u_{\beta}\beta \frac{\partial T_{L}}{\partial \beta} = \frac{D_{T}}{r} \left(\frac{\partial^{2} T_{L}}{\partial \alpha^{2}} + \frac{1}{\alpha} \frac{\partial T_{L}}{\partial \alpha} + \frac{\partial^{2} T_{L}}{\partial \beta^{2}} + \frac{1}{\beta} \frac{\partial T_{L}}{\partial \beta} \right)$$
(3)

where u_{α} and u_{β} are the normal and tangent components of relative velocities between the interface of growing dendritic crystal and the undercooled melt, which are defined as follows:

$$u_{\alpha} = -V(V+U) + \frac{Ug(\alpha)}{\alpha} \tag{4}$$

$$u_{\beta} = (V + U) + U \frac{\mathrm{d}}{\mathrm{d}\alpha} (\alpha g(\alpha)) \tag{5}$$

where U is the incoming fluid flow velocity far from the interface, and $g(\alpha)$ is described by

$$g(\alpha) = \frac{\alpha E_1 \left(\frac{Re\alpha^2}{2}\right)}{E_1 \left(\frac{Re}{2}\right)} - \frac{\exp\left(-\frac{Re}{2}\right) - \exp\left(-\frac{Re\alpha^2}{2}\right)}{Re\alpha E_1 \left(\frac{Re}{2}\right)}$$
(6)

where Re is the Reynolds number defined by $Re=rU/\eta$ and the exponential function $E_1(z)$ is defined by

$$E_1(z) = \int_z^\infty \frac{e^{-t}}{t} dt \tag{7}$$

It is hard to obtain the exact solution of Eq. (3), due to the complexity of the expression of $g(\alpha)$ defined by Eq. (6). In order to discuss the effect of convection in the liquid on the thermal diffusion field, a simplified version of $g(\alpha)=1/\alpha$ is taken. This corresponds to the ideal fluid condition. Then, Eq. (3) can be rewritten as

$$\frac{\partial^{2} T_{L}}{\partial \alpha^{2}} + \left(\frac{1 - 2P_{tf}}{\alpha} + 2P_{t0}\alpha\right) \frac{\partial T_{L}}{\partial \alpha} + \frac{\partial^{2} T_{L}}{\partial \beta^{2}} + \frac{1}{\beta} \frac{\partial T_{L}}{\partial \beta} = 0$$
(8)

where $P_{t0}=P_t+P_{tf}$, P_t is the thermal growth Peclet number defined by $P_t=rV/(2D_T)$, and P_{tf} is the thermal flow Peclet number defined by $P_{tf}=rU/(2D_T)$. In this equation, a term $-2P_{t0}\beta\partial T_L/\partial\beta$ is neglected with the approximation $1/\beta\gg 2P_{t0}\beta$, since the solidification behavior at the tip of dendrite $(\beta=0)$ is only influenced by the regions in the vicinity of $\beta\approx 0$ [23].

By adopting the separation variable method, Eq. (8) is divided into a Bessel equation and a confluent hypergeometric equation. Its solution can be obtained as

$$T(\alpha,\beta) = \int_{0}^{\infty} A_{t}(\lambda) \exp(-P_{t0}\alpha^{2}) \cdot \Phi(1 - P_{tf} + \frac{\lambda^{2}}{4P_{t0}}, 1 - P_{tf}, P_{t0}\alpha^{2}) \cdot J_{0}(\lambda\beta) d\lambda + T_{\infty}$$

$$(9)$$

where $\Phi(a, b, z)$ is the confluen thypergeometric function of the second kind, $J_0(\lambda\beta)$ is the zeroth order Bessel function of the first kind, T_∞ is the temperature of the undercooled melt far from the interface as an integration constant, $A_t(\lambda)$ is a coefficient to be determined, and λ is a constant. Considering the nonisothermal nature of the

interface, caused by the non-planar interface and the crystalline anisotropy, with the isosolutal interface assumption [25], the interface response function can be given as [24]

$$T_{L}(1,\beta) = T_{M} - \frac{Q}{c_{p}} \frac{2d_{0}}{r} f_{1}(\beta) - \tilde{\beta}V f_{2}(\beta) - \left(m_{L}C_{0} - m(V)C_{L}^{*}\right)$$

$$(10)$$

where $T_{\rm L}(1,\beta)$ represents the interfacial temperature, $T_{\rm M}$ is the melting point of binary alloy with the nominal composition C_0 , Q is the latent heat of fusion, c_p is the specific heat capacity, d_0 is the capillary constant, $\tilde{\beta}$ is the kinetic coefficient, $m_{\rm L}$ is the slope of equilibrium liquidus, and $C_{\rm L}^*$ is the solute concentration on the liquid side at the tip. In addition, the kinetic liquidus slope m(V) and the parameters $f_1(\beta)$ and $f_2(\beta)$ are defined as follows with the assumption θ_d =0 and θ_β = π /4 [24]:

$$f_1(\beta) = (1 - a_d)(1 + \beta^2)^{-\frac{1}{2}} + (1 + 7a_d)(1 + \beta^2)^{-\frac{3}{2}} - 8a_d(1 + \beta^2)^{-\frac{7}{2}}$$
(11)

$$f_{2}(\beta) = (1 + a_{\beta})(1 + \beta^{2})^{-\frac{1}{2}} - 8a_{\beta}(1 + \beta^{2})^{-\frac{3}{2}} + 8a_{\beta}(1 + \beta^{2})^{-\frac{5}{2}}$$

$$(12)$$

$$m(V) = \frac{m_{\rm L}}{1 - k_{\rm e}} \left[1 - k(V) + \left(1 - k(V) \right)^2 \frac{V_{\rm n}}{V_{\rm D}} + \ln\left(\frac{k(V)}{k_{\rm e}}\right) \right], \quad V < V_{\rm D}$$

$$(13a)$$

$$m(V) = \frac{m_{\rm L}}{k_{\rm e} - 1} \ln k_{\rm e}, \ V \ge V_{\rm D}$$
 (13b)

$$k(V) = \frac{k_{\rm e}\psi - (V/V_{\rm DI})}{\psi - (V/V_{\rm DI})}, \ V < V_D$$
 (14a)

$$k(V) = 1, \ V \ge V_D \tag{14b}$$

where a_d and a_β are the stiffnesses of anisotropy, $V_{\rm D}$ is the solute diffusive speed in bulk liquid, $V_{\rm n}$ is the interfical normal speed, $k_{\rm e}$ and k are the equilibrium and nonequilibrium partition coefficients, respectively, and $V_{\rm DI}$ is the interfacial solute diffusive velocity, $\psi = 1 - V^2/V_{\rm D}^2$ at $V < V_{\rm D}$ and $\psi = 0$ at $V \ge V_{\rm D}$.

By using the Hankel transform for coordinate β , combined with Eqs. (9) and (10), $A_t(\lambda)$ can be further determined as follows:

$$A_{t}(\lambda) = \left\{ \left[\left(T_{M} - T_{\infty} \right) - \left(m_{L} C_{0} - m(V) C_{L}^{*} \right) \right] \cdot \delta(\lambda) - \frac{Q}{c_{p}} \frac{2d_{0}}{r} F_{1}(\lambda) - \tilde{\beta} V F_{2}(\lambda) \right\} / \left\{ \exp(-P_{t0}\alpha) \cdot \Phi \left(1 - P_{tf} + \frac{\lambda^{2}}{4P_{t0}}, 1 - P_{tf}, P_{t0} \right) \right\}$$

$$(15)$$

where $\delta(\lambda)$ is the delta function. $F_1(\lambda)$ and $F_2(\lambda)$ are defined by [23]

$$F_{1}(\lambda) = (1 - a_{d}) + \left(1 + \frac{27}{5}a_{d}\right)\lambda - \frac{8}{5}a_{d}\lambda^{2} - \frac{8}{15}a_{d}\lambda^{3}$$
(16)

$$F_2(\lambda) = \left(1 + a_\beta\right) - \frac{16}{3}a_\beta\lambda + \frac{8}{3}a_\beta\lambda^2 \tag{17}$$

Additionally, the thermal transport balance equation is adopted at the nonisothermal solid—liquid interface:

$$V_{\rm n}(\beta)Q = -K_{\rm L}\bar{n} \cdot \nabla T_{\rm L}(\alpha,\beta)\Big|_{\alpha=1} \tag{18}$$

where K_L is the thermal conductivity in the liquidin the absence of melt convection, and \bar{n} is the unit vector normal to the interface. Substituting the temperature field described by Eq. (9) into the conservation equation, Eq. (18), the following relationship at the tip (β =0) can be finally given as follows:

$$\Delta T = \frac{Q}{c_p} \text{Iv}(P_{t}, P_{tf}) + \frac{Q}{c_p} \frac{2d_0}{r} N_1(P_{t}, P_{tf}) + \tilde{\beta} V N_2(P_{t}, P_{tf}) + m_L C_0 - m(V) C_L^*$$
(19)

where the new Ivantsov function $Iv(P_t, P_{tf})$ and the parameters $N_1(P_t, P_{tf})$ and $N_2(P_t, P_{tf})$ are defined by

$$Iv(P_{t}, P_{tf}) = \frac{P_{t}}{P_{t0}} \frac{\Phi(1 - P_{tf}, 1 - P_{tf}, P_{t0})}{\Phi(1 - P_{tf}, 2 - P_{tf}, P_{t0})} = P_{t}e^{P_{t0}} \int_{1}^{\infty} \frac{\exp(-P_{t0}\alpha)}{\alpha^{1-P_{tf}}} d\alpha$$

$$N_{1}(P_{t}, P_{tf}) = \frac{\Phi(1 - P_{tf}, 1 - P_{tf}, P_{t0})}{\Phi(1 - P_{tf}, 2 - P_{tf}, P_{t0})}.$$

$$P_{1}(P_{t}, P_{tf}) = \frac{\Phi(1 - P_{tf}, 1 - P_{tf}, P_{t0})}{\Phi(1 - P_{tf}, 2 - P_{tf}, P_{t0})}.$$

$$\int_{0}^{\infty} e^{-\lambda} \frac{F_{1}(\lambda)}{2} \frac{\Phi(1 - P_{tf} + \lambda^{2} / (4P_{t0}), 2 - P_{tf}, P_{t0})}{\Phi(1 - P_{tf} + \lambda^{2} / (4P_{t0}), 1 - P_{tf}, P_{t0})} d\lambda$$
(21)

$$N_2(p_{t}, P_{tf}) = \frac{\Phi(1 - P_{tf}, 1 - P_{tf}, P_{t0})}{\Phi(1 - P_{tf}, 2 - P_{tf}, P_{t0})}$$

$$\int_{0}^{\infty} e^{-\lambda} F_{2}(\lambda) \frac{\Phi(1 - P_{\text{tf}} + \lambda^{2} / (4p_{\text{t}}), 2 - P_{\text{tf}}, p_{\text{t}})}{\Phi(1 - P_{\text{tf}} + \lambda^{2} / (4p_{\text{t}}), 1 - P_{\text{tf}}, p_{\text{t}})} d\lambda$$
(22)

Here, a relationship $\Phi(a, a, z)/\Phi(a, a+1, z)=$ $ze^{z}\int_{0}^{\infty}e^{-zt}t^{-a}dt$ is used, which can be demonstrated mathematically.

As the value of $g(\alpha)$ is in the range of (0, 1) and is monotonically decreasing with α , there are two limit cases for the effect of convection on the thermal diffusion in liquid phase. $g(\alpha)\equiv 1$ represents the condition that there is no convection in the liquid. With this assumption, the present result is reduced to the previous one [24]. Under another limit condition, $g(\alpha)\equiv 0$, one can obtain the same expression as described by Eq. (19), in which related parameters are redefined as follows:

$$Iv(P_{t}, P_{tf}) = \frac{P_{t}}{P_{t0}} \frac{\Phi(1, 1, P_{t0})}{\Phi(1, 2, P_{t0})} = P_{t}e^{P_{t0}} \int_{1}^{\infty} \frac{\exp(-P_{t0}\alpha)}{\alpha} d\alpha$$
(23)

$$N_1(P_t, P_{tf}) = \frac{\Phi(1, 1, P_{t0})}{\Phi(1, 2, P_{t0})}$$

$$\int_{0}^{\infty} e^{-\lambda} \frac{F_{1}(\lambda)}{2} \frac{\Phi(1+\lambda^{2}/(4P_{t0}), 2, P_{t0})}{\Phi(1+\lambda^{2}/(4P_{t0}), 1, P_{t0})} d\lambda (24)$$

$$N_2(P_t, P_{tf}) = \frac{\Phi(1, 1, P_{t0})}{\Phi(1, 2, P_{t0})}$$

$$\int_{0}^{\infty} e^{-\lambda} F_{2}(\lambda) \frac{\Phi(1+\lambda^{2}/(4P_{t0}), 2, P_{t0})}{\Phi(1+\lambda^{2}/(4P_{t0}), 1, P_{t0})} d\lambda (25)$$

2.2 Solutal transport in liquid

For solutal transport in the liquid, the isosolutal assumption along the solid-liquid interface has been shown to be reasonable approximation [22]. With this assumption the interfacial solute composition at the tip is given by ALEXANDROV and GALENKO [28] as

$$C_{\rm L}^* = \frac{C_0}{1 - (1 - k(V)) \operatorname{Iv}(P_{\rm c}, P_{\rm cf})}$$
 (26)

where P_c is the solute growth Peclet number defined by $P_c=rV/(2D_L)$ (where D_L is the solute diffusivity in the liquid), and P_{cf} is the solute flow

Peclet number defined by $P_{\rm cf}=rU/(2D_{\rm L})$. At the given parabolic coordinate system (α, β, φ) , $Iv(P_{\rm c}, P_{\rm cf})$ is defined as

$$\operatorname{Iv}(P_{c}, P_{cf}) = \int_{1}^{\infty} \exp\left[2P_{cf} \int_{1}^{\alpha} g(\alpha) d\alpha - P_{c0} \alpha^{2}\right] \frac{2d\alpha}{\alpha}$$
(27)

where P_{c0} is defined by $P_{c0}=P_{c}+P_{cf}$.

Considering the relaxation effect of local nonequilibrium solute diffusion in bulk liquid, the interfacial solute composition at the tip can be rewritten as [9,11]

$$C_{\rm L}^* = \frac{C_0}{1 - (1 - k(V)) \operatorname{Iv}(P_{\rm c}, P_{\rm cf})}, \ V < V_D$$
 (28a)

$$C_{\rm L}^* = C_0, \ V \ge V_{\rm D}$$
 (28b)

Similar to the thermal diffusion, there are also two limit cases for the solute diffusion. One is with the assumption $g(\alpha)\equiv 1$, i.e. the condition ignoring the effect of convection on solute diffusion in the liquid. The other limit case is with the assumption of $g(\alpha)\equiv 0$. Under this condition, Eq. (27) can be re-solved as

$$Iv(P_{c}, P_{cf}) = \frac{P_{c}}{P_{c0}} \frac{\Phi(1, 1, P_{c0})}{\Phi(1, 2, P_{c0})} = P_{c} e^{P_{c0}} \int_{1}^{\infty} \frac{\exp(-P_{c0}\alpha)}{\alpha} d\alpha$$
 (29)

2.3 Morphological stability criterion

The analysis of solid-liquid interface morphological stability should be made to uniquely determine solidification behavior with steady state dendritic growth. Taking into account the interfacial nonisothermal nature, the microscopic solvability theory can give a correlation between the tip radius of curvature r and the interfacial migration velocity V at a given bath undercolling ΔT . According to Ref. [28], the selection criterion derived from microscopic solvability theory is described as

$$\sigma^* = \frac{\sigma_0 a_d^{-7/4}}{1 + b \left(\beta^{-3/4} \alpha_0 \left(Re\right)\right)^{11/14}} \cdot \left(\xi_t + \frac{2m(V)C_L(1 - k(V)D_T)}{D_L T_O} \xi_c\right), \ V \ge V_D$$
 (30a)

$$\sigma^* = \frac{\sigma_0 a_d^{-7/4}}{1 + b \left(\beta^{-3/4} \alpha_0 \left(Re\right)\right)^{11/14}} \xi_t, \ V \ge V_D$$
 (30b)

where σ^* is defined by $\sigma^*=2D_{\rm T}d_0/(r^2V)$, σ_0 is the selection constant, , T_Q is defined by $T_Q=Q/c_p$, and the other parameters are defined as follows:

$$\xi_{t} = \left[1 + a_{1}\sqrt{a_{d}}P_{t}\left(1 + a_{1}\sqrt{a_{d}}P_{t}\left(1 + \delta_{0}D_{T}\beta_{0}/d_{0}\right)\right)\right]^{-2}$$
(31)

$$\xi_{c} = \left[1 + a_{2} \sqrt{a_{d}} P_{c}^{*} \left(1 + \delta_{0} D_{L} \beta_{0} / d_{0CD} \right) \right]^{-2}$$
 (32)

$$\alpha_0 \left(Re \right) = \frac{ad_0 U}{4\rho V p} + \frac{ad_0 U D_{\rm T}}{2\rho V p D_{\rm L}} \tag{33}$$

where a_1 is a constant defined by σ_0 $(a_1=(8\sigma_0/7)^{1/2}(3/56)^{3/8})$, $a_2=\sqrt{2}a_1$, $P_{\rm c}^*$ is defined by $P_{\rm c}^*=P_{\rm c}/\sqrt{\psi}$, $\delta_0=1$, $d_{\rm OCD}$ is the chemical capillary length, and the parameters $\alpha(Re)$ and p are defined by

$$\alpha(Re) = \frac{\exp(-Re/2)}{E_1(Re/2)} \tag{34}$$

$$p = 1 + \frac{2m(V)C_{L}^{*}(1 - k(V))D_{T}}{D_{L}Q/c_{p}}$$
(35)

Then being derived from Eq. (31), the tip radius of curvature r can be obtained as

$$r = \frac{d_0 T_{Q} \left[1 + b \left(a_d^{-3/4} \alpha_0 \left(Re \right) \right)^{11/14} \right]}{\sigma_0 a_d^{7/4}} \cdot \frac{1}{\left(T_{Q} \xi_t P_t + 2m(V) C_L \left(k(V) - 1 \right) \xi_c P_c^* \right)}, \ V < V_D$$
(36a)

$$r = \frac{d_0 T_Q \left[1 + b \left(a_d^{-3/4} \alpha_0 \left(Re \right) \right)^{11/14} \right]}{\sigma_0 a_d^{7/4}} \frac{1}{T_Q \xi_t P_t}, \ V \ge V_D$$
(36b)

Up to now, considering forced flow in the fluid, the entire free dendrite growth model has been described. By solving Eqs. (19), (28) and (36) simultaneously, with any given bath undercooling ΔT , one can determine the solidification behavior, uniquely.

3 Results and discussion

In this section, model comparisons were made to analyze the effect of convection on thermal diffusion and solutal diffusion. Experimental comparison was also made for the $Cu_{70}Ni_{30}$ alloy. The numerical results are shown in Figs. 1–6. The thermo-physical data, used in the present computations, are listed in Table 1. In order to express more clearly, the distinction between these models discussed in the present work is shown in Table 2.

Table 1 Thermo-physical data for Cu₇₀Ni₃₀ alloy used in model computations

Parameter	Value
Solidification temperature, $T_{\rm M}/{\rm K}$	1513 [22]
Heat of fusion, $Q/(J \cdot kg^{-1})$	2.317×10^{5} [24]
Specific heat capacity, $c_p/(J \cdot kg^{-1} \cdot K^{-1})$	576
Anisotropic capillary length, d_0 /m	6.2×10^{-10}
Chemical capillary length, $d_{0\mathrm{CD}}/\mathrm{m}$	3.48×10^{-9}
Diffusion coefficient, $D_{\rm L}/({\rm m}^2\cdot{\rm s}^{-1})$	$6.0 \times 10^{-9} [24]$
Thermal diffusivity, $a_L/(m^2 \cdot s^{-1})$	3×10^{-6} [24]
Interfacial diffusion speed, $V_{\rm Dl}/({\rm m\cdot s}^{-1})$	10 [24]
Diffusion speed in bulk liquid, $V_D/(m \cdot s^{-1})$	19 [24]
Liquidus slope, $m_L/(K \cdot at.\%^{-1})$	-4.38 [24]
Partition coefficient, $k_{\rm e}$	0.81 [24]
Coefficient of growth, $\tilde{\beta}/(s \cdot K \cdot m^{-1})$	0.588
Stiffness of surface energy anisotropy, a_d	0.25
Stiffness of kinetic anisotropy, a_{β}	0.25
Selection constant, σ_0	1.5
Velocity of force convection, $U/(\text{m}\cdot\text{s}^{-1})$	0.3
Coefficient of fluid viscosity, $\eta/(m^2 \cdot s^{-1})$	0.5×10^{-7}

3.1 Effect of convection on thermal diffusion

The dendritic tip temperature T_i as function of the bath undercooling ΔT is shown in Fig. 1, for three models considering different expressions of $g(\alpha)$.

Table 2 Definition of $g(\alpha)$ used in different models

	0 . ,	
No.	Thermal diffusion	Solute diffusion
Limit case 1	<i>g</i> (α)≡1	<i>g</i> (α)≡1
Limit case 2	$g(\alpha)\equiv 0$	<i>g</i> (α)≡1
Ideal fluid case	$g(\alpha)=1/\alpha$	<i>g</i> (α)≡1
Limit case 3	<i>g</i> (α)≡1	$g(\alpha)=0$
Nonideal fluid case	<i>g</i> (α)≡1	$g(\alpha)$ defined by Eq. (6)

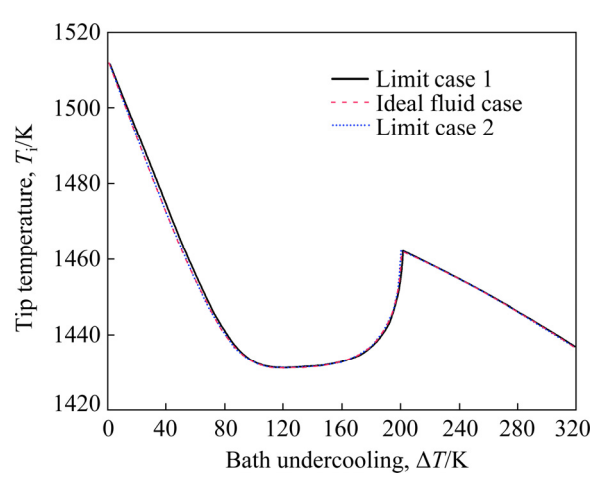


Fig. 1 Evolution of tip temperature as function of bath undercooling ΔT for Cu₇₀Ni₃₀ alloy

As the value of $g(\alpha)$ is in the range of (0, 1) and is monotonically decreasing with α , there are two limit cases for the effect of convection on the thermal diffusion in liquid phase. As shown in Table 2, limit case 1 represents the model with assumption of $g(\alpha) \equiv 1$, and this is the condition that there is no convection in the liquid. Another limit case, called limit case 2, denotes the model with assumption of $g(\alpha) \equiv 0$. It is a limiting condition that the influence of the convection on thermal diffusion is the most remarkable. The ideal fluid case means the model with the assumption of $g(\alpha)=1/\alpha$. It should be stressed that in order to focus on the discussion about the effect of convection on thermal diffusion, different expressions of $g(\alpha)$ are only adopted in the description of thermal diffusion, while the same equations were adopted in the description of solutal diffusion, Eqs. (27) and (28) with $g(\alpha) \equiv 1$, as well as morphological stability criterion, Eq. (36), for the three models. This can be seen from Table 2 more clearly. Figure 1 shows that there are slight differences of the dendritic tip temperatures between these models at low bath undercoolings while the differences are more negligible at high bath undercoolings.

As well know, the total undercooling ΔT can be divided into the following five parts: the thermal undercooling $\Delta T_{\rm T} = T_{\rm M} - T_{\infty}$, the constitutional undercooling $\Delta T_{\rm C} = m(V)(C_{\rm L}^* - C_0)$, the undercooling due to the kinetic liquidus line which deviates from the equilibrium position $\Delta T_{\rm N} = (m_{\rm L} - m(V))C_0$, the curvature undercooling $\Delta T_{\rm R} = (Q/c_p)2d_0/r$ and the kinetic undercooling $\Delta T_{\rm K} = \tilde{\beta}V$. So, we have $\Delta T = \Delta T_{\rm T} + \Delta T_{\rm C} + \Delta T_{\rm N} + \Delta T_{\rm R} + \Delta T_{\rm K}$.

Based on this relationship and the result given by the present model, Eq. (19), one can further determine the thermal undercooling $\Delta T_{\rm T}$ as $\Delta T_{\rm T} = \text{Iv} Q/c_p + \Delta T_{\rm R}(N_1 - 1) + \Delta T_{\rm K}(N_2 - 1)$ (where N_1 is the parameter mentioned above as $N_1(P_t, P_{tf})$; N_2 is the parameter mentioned above as $N_2(P_t, P_{tf})$). Thus, the difference between the tip temperatures T_1^* predicted by the three models discussed above can be analyzed through the values of the Ivantsov function (Iv) and the parameters N_1 and N_2 , due to the relation $\Delta T_{\rm T} = T_{\rm L}^* - T_{\infty}$. The values of the Ivantsov function (Iv) and the parameters N_1 and N_2 as functions of both Peclet number Pt and undercooling ΔT are shown in Figs. 2 and 3, respectively. It can be seen from Fig. 2 that the values of Iv for the three conditions are almost equal to each other. This means that the effect of convection on thermal diffusion with the isothermal interface assumption is ignorable $(N_1=N_2=1)$. Under the nonisothermal interface condition, the parameters N_1 and N_2 are not constantly equal to 1. So, the difference between the tip temperatures T_1^* predicted by the three models is mainly caused by the parameters N_1 and N_2 . As shown in Fig. 3, at low undercoolings ΔT , the value of parameter N_2 given by limit case 1 has an obvious deviation from that predicted by limit case 2, while there is a relatively small difference between the parameters N_1 . However, it is just the value of parameter N_1 that plays an important role in determining the difference between the tip temperatures T_1^* predicted by the three models. This is because the curvature undercooling ΔT_R is much larger than the kinetic undercooling $\Delta T_{\rm K}$, at low bath undercooling ΔT , in the relationship $\Delta T_{\rm T} = \text{Iv} Q/c_p + \Delta T_{\rm R}(N_1 - 1) +$ $\Delta T_{\rm K}(N_2-1)$. Under this condition, the value of parameter N_2 almost does not influence the difference between $T_{\rm L}^*$. Therefore, considering the small difference between the values of N_1 , the effect of convection on thermal diffusion is also very slight under the condition with nonisothermal solid-liquid interface. Additionally, in Fig. 4 it can also be seen that there is a very slight deviation of the interfacial migration velocity predicted by limit case 1 from that calculated by limit case 2, especially at high undercooling.

There are several parameters which can influence the effect of convection on thermal diffusion, such as the velocity of convection U, the coefficient of the fluid viscosity η and the stiffness

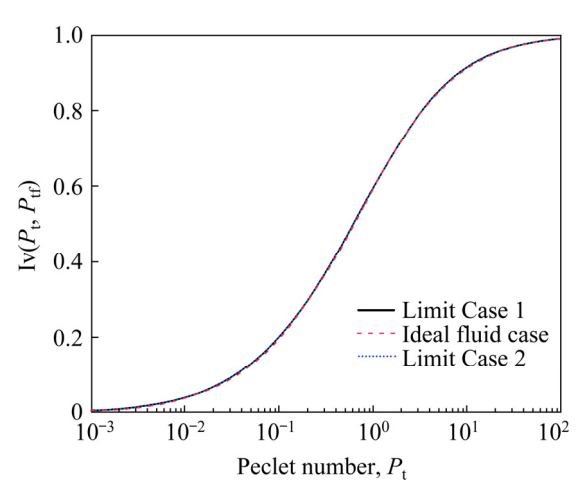


Fig. 2 Ivantsov function on thermal diffusion $Iv(P_t, P_{tf})$ as function of thermal Peclet number P_t , at given velocity of forced convection U=0.3 m/s

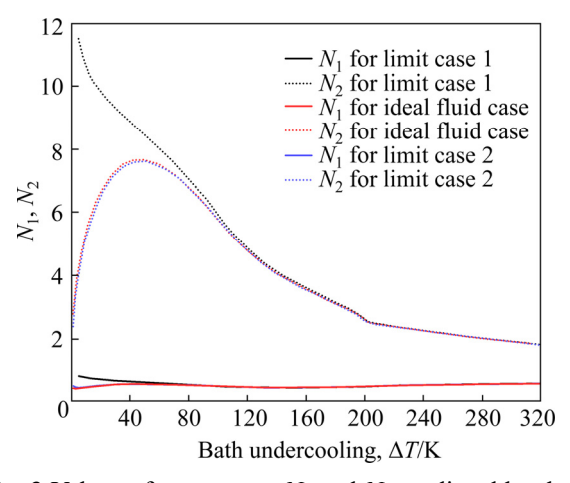


Fig. 3 Values of parameters N_1 and N_2 predicted by three models, as function of bath undercooling ΔT for Cu₇₀Ni₃₀ alloy

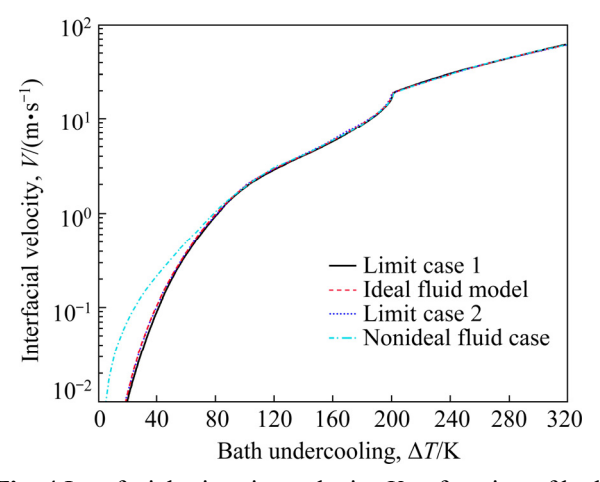


Fig. 4 Interfacial migration velocity V as function of bath undercooling ΔT for $\text{Cu}_{70}\text{Ni}_{30}$ alloy

of anisotropy a_d . The faster the velocity of convection U is or the smaller the coefficient of the

fluid viscosity η is, the more remarkable the influence of convection on solute diffusion is. Besides these two factors, the anisotropy strength a_d is also a factor that can determine the degree of the convection effect. As described by Eqs. (16) and (21), the value of N_1 depends on the anisotropy strength a_d . Taking these parameters given in Table 1, the effect of convection on thermal diffusion is slight enough to be ignored. Furthermore, as discussed in the next section, the effect of convection on solute diffusion is remarkable compared with the ignorable effect of convection on thermal diffusion.

Based on above discussion, it is also concluded that the effect of nonisothermal nature of the solid-liquid interface is comparable with the effect of convection on thermal diffusion. However, it should be stressed that above discussion is made with the assumption θ_d =0 and θ_β = π /4 as well as a set of parameters given in Table 1. Under other conditions, the effect of non-isothermality may be obvious or even remarkable [23–27]. For example, as discussed in Ref. [27], the effect of non-isothermality is not ignorable and should be taken into account, under the condition that θ_d = π /4 or a_d decreases to 0.1.

3.2 Effect of convection on solute diffusion

In this section, three cases are used for comparative analysis, including limit case 1, limit case 3 and nonideal fluid case. Limit case 1 is the one mentioned above that there is no convection in the liquid. $g(\alpha) \equiv 1$ is adopted for limit case 1 in the equations describing both thermal diffusion and solute diffusion in the liquid phase. Limit case 3 represents the model with $g(\alpha) \equiv 0$ in Eqs. (28) and (30), for solute diffusion, which means the maximum limit of the influence of convection on solute diffusion. The nonideal fluid case represents the model, in which $g(\alpha)$ is defined by Eq. (6) for Eqs. (27) and (28) in the solutal transport (Section 2.2). In order to focus on the discussion about the effect of convection on solute diffusion, the same expressions of $g(\alpha) \equiv 1$ are adopted in the description of thermal diffusion (see also the column "Thermal diffusion" in Table 2). That is to say, in this section it is assumed that the influence of convection on thermal diffusion in liquid is neglected completely in all of the three cases.

As shown in Fig. 4, there is an obvious

distinction between the nonideal fluid case and the limit case 1 for the interfacial velocity at low bath undercooling. In contrast, as discussed in Section 3.1, the deviation of the interfacial velocity predicted by limit case 2 from that calculated by limit case 1 is very slight. It is indicated that the effect of convection on solute diffusion is greater than that on thermal diffusion with a set of parameters given in Table 1. This is due to the fact that solute diffusion coefficient is usually three orders of magnitude less than thermal diffusion coefficient. Therefore, the solute diffusion is remarkably slower compared to thermal diffusion. It is just the slower diffusion that leads to more obvious influence of the forced convection on the solutal diffusion compared with the thermal diffusion. This can also be understood by using the solute diffusion scale $l_{\rm C}$ and the hydrodynamic spatial scale $l_{\rm H}$, which are defined as $l_{\rm C}=2D_{\rm L}/V$ and $l_{\rm H} = \eta/U$, respectively [35]. The ratio of $l_{\rm C}$ to $l_{\rm H}$ ($l_{\rm C}/l_{\rm H}$) is shown in Fig. 5, as a function of the bath undercooling. It is indicated that the value of $l_{\rm C}$ is comparable with the value of $l_{\rm H}$ at low undercoolings. Thus, the effect of forced convection on the solutal diffusion is obvious [35].

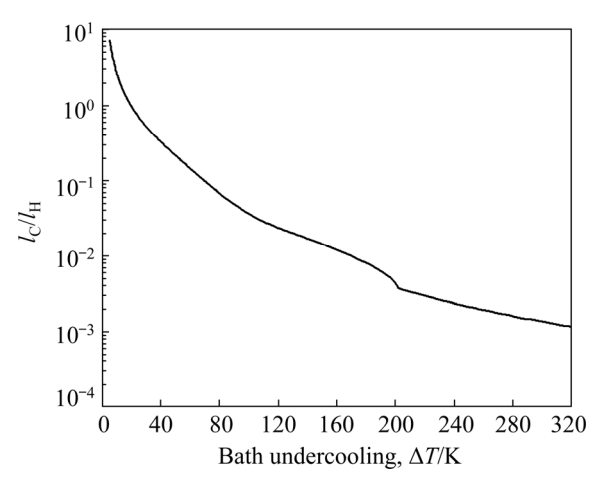


Fig. 5 Ratio of solutal length scale $l_{\rm C}$ to hydrodynamic length scale $l_{\rm H}$ as function of bath undercooling ΔT for ${\rm Cu}_{70}{\rm Ni}_{30}$ alloy

In order to further demonstrate the effect of convection on solute diffusion, the tip solute concentration C_L^* of the dendrite as a function of the bath undercooling ΔT is shown in Fig. 6, for different models including the nonideal fluid cases with η =5×10⁻⁸ m²/s and η =5×10⁻¹⁰ m²/s. Firstly, it can be seen that the larger the coefficient of viscosity η is, the slighter the effect of the

convection on solute diffusion is. Secondly, the forced convection results in the lower tip solutal concentrations C_L^* on the liquid side compared with the condition that there is not forced convection. Thus, the forced convection can depress solute segregation at the solid-liquid interface. Thirdly, as indicated by Fig. 5, the effect of convection on solute diffusion is very slight and can further be ignored at high bath undercooling, since the solute trapping or even complete solute trapping occurs. Therefore, the effect of convection on solute diffusion should be taken into account in modeling free dendritic growth, under the condition that there exists forced convection, especially at low bath undercoolings.

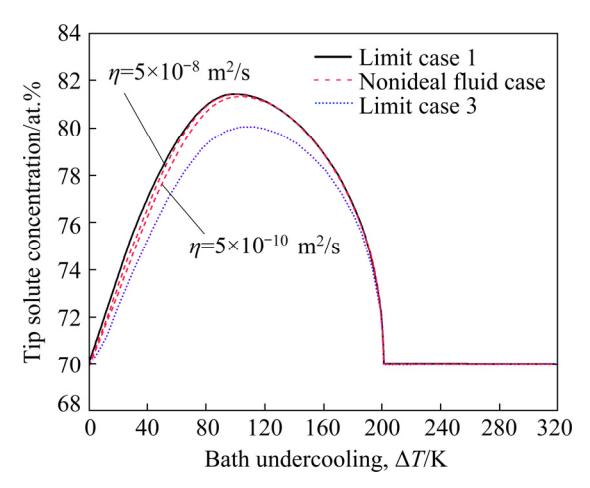


Fig. 6 Evolution of tip solute concentration (mole fraction) on liquid side as function of bath undercooling, for $Cu_{70}Ni_{30}$ alloy

3.3 Experimental comparison

An experimental comparison for the interfacial migration velocity V versus the bath undercooling ΔT for the Cu₇₀Ni₃₀ alloy is shown in Fig. 7 [36]. As discussed above, the effect of convection on solute diffusion is remarkable compared with the ignorable effect of convection on thermal diffusion. Thus, in Fig. 7, the interfacial velocity V is predicted by the present model with the nonideal fluid case shown in Table 2. The related thermophysical parameters are shown in Table 1. In addition, as one of the series of models [20–24], the present model also takes into account the nonisothermal nature of the solid-liquid interface caused by curved interface and crystalline anisotropy and takes the isosolutal interface assumption. It is indicated that the present model can give a satisfying description to the experiment data, especially at low bath undercoolings. One of the main reasons lies in the fact that the present model introduces the effect of the forced convection on solutal diffusion. It can be further supported by Fig. 4, in which the interfacial migration velocity V predicted by the present model with nonideal fluid case is obviously faster than that predicted by the one ignoring the effect of convection.

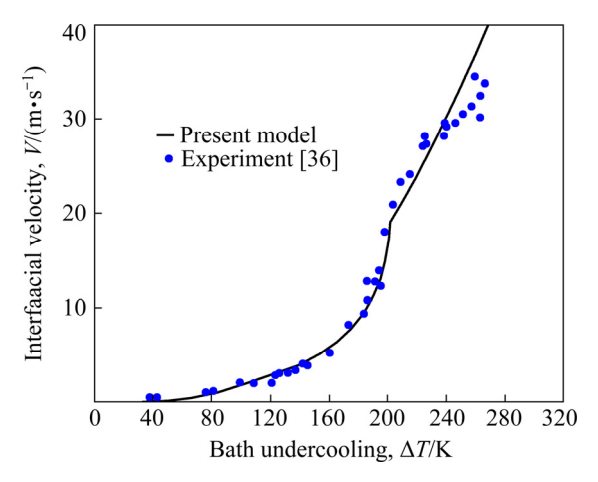


Fig. 7 Comparison of experimental and predicted results of interfacial migration velocity V as function of bath undercooling ΔT for Cu₇₀Ni₃₀ alloy

4 Conclusions

- (1) The larger the coefficient of viscosity, the slighter the effect of the convection on solute diffusion. The forced convection can depress solute segregation at the solid—liquid interface.
- (2) Model comparison indicates that the effect of convection on solute diffusion is remarkable compared with the ignorable effect of convection on thermal diffusion, at low bath undercooling. At high bath undercooling, the effect of convection is very slight.
- (3) Experimental comparison shows that the present model can give a satisfying description to the experimental data for the Cu₇₀Ni₃₀ alloy, especially at low bath undercoolings, benefiting by introducing the effect of forced convection on solutal diffusion.

Acknowledgments

The authors are grateful for the financial supports from the National Natural Science Foundation of China (No. 51671075), the Heilong-jiang Postdoctoral Fund for Scientific Research Initiation (No. LBH-Q16118), and the Fundamental

Research Foundation for Universities of Heilongjiang Province, China (No. LGYC2018-JC004).

References

- FU Heng-zhi, XIE Fa-qin. Solidification characteristics of near rapid and supercooling directional solidification [J]. Transactions of Nonferrous Metals Society of China, 1999, 9: 659–667
- [2] CHEN Shou-dong, CHEN Jing-chao. Simulation of microstructures in solidification of aluminum twin-roll casting [J]. Transactions of Nonferrous Metals Society of China, 2012, 22: 1452–1456.
- [3] YAN Xue-wei, GUO Xiong, LIU Yan-ling, GONG Xiu-fang, XU Qing-yan, LIU Bai-cheng. Numerical simulation of dendrite growth in Ni-based superalloy casting during directional solidification process [J]. Transactions of Nonferrous Metals Society of China, 2019, 29: 338–348.
- [4] ZHANG Ang, DU Jing-lian, GUO Zhi-peng, WANG Qi-gui, XIONG Shou-mei. Dendritic growth under natural and forced convection in Al-Cu alloys: From equiaxed to columnar dendrites and from 2D to 3D phase-field simulations [J]. Metallurgical and Materials Transactions B, 2019, 50(3): 1514–1526.
- [5] ALEXANDROVA D V, TITOVA E A, GALENKO P K. A shape of dendritic tips at high Péclet numbers [J]. Journal of Crystal Growth, 2019, 515: 44–47.
- [6] REUTHER K, GALENKO P K, RETTENMAYR M. Dynamic instability of the steady state of a planar front during non-equilibrium solidification of binary alloys [J]. Journal of Crystal Growth, 2019, 506: 55–60.
- [7] LIPTON J, GLICKSMAN M E, KURZ W. Dendritic growth into undercooled alloy melts [J]. Materials Science and Engineering, 1984, 65: 57–63.
- [8] BOETTINGER W J, CORIELL S R, TRIVEDI R. Rapid solidification processing: Principles and technologies IV [M]. Baton Rouge, LA: Claitor's, 1988: 13–24.
- [9] SOBOLEV S L. Rapid solidification under local nonequilibrium conditions [J]. Physical Review E, 1997, 55: 6845–6854.
- [10] GALENKO P K, DANILOV D A. Local nonequilibrium effect on rapid dendritic growth in a binary alloy melts [J]. Physics Letters A, 1997, 235: 271–280.
- [11] DIVENUTI A G, ANDO T. A free dendritic growth model accommodating curved phase boundaries and high Peclet number conditions [J]. Metallurgical and Materials Transactions A, 1998, 29: 3047–3056.
- [12] GALENKO P K, DANILOV D A. Model for free dendritic alloy growth under interfacial and bulk phase nonequilibrium conditions [J]. Journal of Crystal Growth, 1999, 197: 992–1002.
- [13] WANG Hai-feng, LIU Feng, CHEN Zheng, YANG Gen-cang, ZHOU Yao-he. Analysis of non-equilibrium dendrite growth in a bulk undercooled alloy melt: Model and application [J]. Acta Materialia, 2007, 55: 497–506.
- [14] LI Shu, ZHANG Jiong, WU Ping. Analysis for free dendritic growth model applicable to nondilute alloys [J]. Metallurgical and Materials Transactions A, 2012, 43:

- 3748–3754.
 [15] TURNBULL D. On the relation between crystallization rate and liquid structure [1]. Journal of Physical Chemistry, 1962.
- [15] TURNBULL D. On the relation between crystallization rate and liquid structure [J]. Journal of Physical Chemistry, 1962, 66: 609–613.
- [16] IVANTSOV G P. Temperature field around spherical, cylindrical, and needle-shaped crystals which grow in supercooled melts [J]. Doklady Akademii nauk SSSR, 1947, 58: 567–569.
- [17] IVANTSOV G P. On the growth of a spherical or a needlelike crystal of a binary alloy [J]. Doklady Akademii nauk SSSR, 1952, 83: 573–576.
- [18] MULLINS W W, SEKERKA R F. Stability of a planar interface during solidification of a dilute binary alloy [J]. Journal of Applied Physics, 1964, 35: 444–451.
- [19] KOTLER G R, TARSHIS L A. An extension to the analysis of dendritic growth in pure systems [J]. Journal of Crystal Growth, 1969, 5: 90–98.
- [20] LI Shu, GU Zhi-hui, LI Da-yong, LIU Shu-cheng, CHEN Ming-hua, FENG Yu. Analysis for free dendritic growth model incorporating the nonisothermal nature of solid—liquid interface [J]. Physics Letters A, 2015, 379: 237–240.
- [21] LI Shu, LI Da-yong, LIU Shu-cheng, GU Zhi-hui, LIU Wei, HUANG Jian-wei. An extended free dendritic growth model incorporating the nonisothermal and nonisosolutal nature of the solid-liquid interface [J]. Acta Materialia, 2015, 83: 310–317.
- [22] LIU Shu-cheng, LI Shu, LIU Feng. Analysis of free dendritic growth considering both relaxation effect and effect of nonisothermal and nonisosolutal interface [J]. International Journal of Heat and Mass Transfer, 2019, 134: 51–57.
- [23] LIU Shu-cheng, LIU Li-hua, LI Shu, WANG Jin-zhong, LIU Wei. Analysis for free dendritic growth model based on nonisothermal interface and microscopic solvability theory [J]. Transactions of Nonferrous Metals Society of China, 2019, 29: 601–607.
- [24] LIU Shu-cheng, LIU Li-hua, LI Shu, WANG Jin-zhong, LIU Wei. Free dendritic growth model for binary alloy based on microscopic solvability theory and nonisothermal nature caused by anisotropy and curved interface [J]. Journal of Crystal Growth, 2020, 532: 125417.
- [25] MCFADDEN G B, CORIELL S R. The effect of fluid flow due to the crystal-melt density change on the growth of a parabolic isothermal dendrite [J]. Journal of Crystal Growth, 1986, 74: 507–512.
- [26] BENAMAR M, BOUISSOU P H. An exact solution for the shape of a crystal growing in a forced flow [J]. Journal of Crystal Growth, 1988, 92: 97–100.
- [27] FUNKE O, PHANIKUMAR G, GALENKO P K, CHERNOVA L, REUTZEL S, KOLBE M, HERLACH D M. Dendrite growth velocity in levitated undercooled nickel melts [J]. Journal of Crystal Growth, 2006, 297: 211–222.
- [28] ALEXANDROV D V, GALENKO P K. Dendrite growth under forced convection: Analysis methods and experimental tests [J]. Physics Uspekhi, 2014, 57: 771–786.
- [29] ALEXANDROV D V, GALENKO P K. Selection criterion of stable dendritic growth at arbitrary Peclet numbers with convection [J]. Physical Review E, 2013, 87: 062403.
- [30] ALEXANDROV D V, GALENKO P K. Thermo-solutal and

- kinetic regimes of an anisotropic dendrite growing under forced convective flow. Phys [J]. Physical Chemistry Chemical Physics, 2015, 17: 19149.
- [31] ALEXANDROV D V, GALENKO P K. Selected mode for rapidly growing needle-like dendrite controlled by heat and mass transport [J]. Acta Materialia, 2017, 137: 64–70.
- [32] MEIRMANOV A M. The Stefan problem [M]. Berlin: Springer, 1992.
- [33] GUPTA S C. Classical Stefan problem [M]. Amsterdam: Elsevier, 2003.
- [34] TRIVEDI R, KURZ W. Dendritic growth [J]. International Materials Reviews, 1994, 39: 49–74.
- [35] GALENKO P K, REUTHER K, KAZAK O V, ALEXANDROV D V, RETTENMAYR M. Effect of convective transport on dendritic crystal growth from pure and alloy melts [J]. Applied Physics Letters, 2017, 111: 031602.
- [36] HERLACH D M, FEUERBACHER B. Non-equilibrium solidification of undercooled metallic melts [J]. Advances in Space Research, 1991, 11: 255–262.

同时考虑界面非等温特性和对流影响的 二元合金自由枝晶生长模型

刘书诚1, 刘礼华1, 李 述2,3, 王金忠1

- 1. 哈尔滨工业大学 材料科学与工程学院,哈尔滨 150001;
 - 2. 哈尔滨理工大学 理学院,哈尔滨 150080;
- 3. 哈尔滨理工大学 黑龙江省量子调控重点实验室,哈尔滨 150080

摘 要:在同时考虑界面非等温性质以及强制对流影响的情况下,提出二元合金的扩展自由枝晶生长模型。模型对比表明:由于溶质扩散系数通常比热扩散系数小3个数量级,当低过冷时,对流对溶质扩散的影响比其对热扩散的影响更强烈。当高过冷时,对流对枝晶生长的影响很小。此外,本模型能够对现有 Cu₇₀Ni₃₀ 合金实验数据给出一致的描述,特别是在低过冷时。这得益于当前模型获得了比忽略对流影响的模型更快的界面迁移速率。 关键词:建模:枝晶凝固;二元合金;非等温界面;对流

(Edited by Wei-ping CHEN)